β-arrestin-dependent and -independent endosomal G protein activation by the vasopressin type 2 receptor

Carole Daly[1], Akim Abdul Guseinov[2], Hyunggu Hahn[3,4], Adam Wright[1], Irina G. Tikhonova[2], Alex Rojas Bie Thomsen[3,4], Bianca Plouffe[1]

[1] Wellcome-Wolfson Institute for Experimental Medicine, School of Medicine, Dentistry and Biomedical Sciences, Queen's University Belfast, Belfast, UK.
[2] School of Pharmacy, Queen's University Belfast, Belfast, UK.
[3] Department of Molecular Pathobiology, New York University College of Dentistry, New York, USA.
[4] NYU Pain Research Center, New York University College of Dentistry, New York, USA.

Correspondence:
e-mail: b.plouffe@qub.ac.uk; art8@nyu.edu

ABSTRACT

The vasopressin type 2 receptor (V_2R) is an essential GPCR in renal regulation of water homeostasis. Upon stimulation, the V_2R activates $G\alpha_s$ and $G\alpha_{q/11}$, which is followed by robust recruitment of β-arrestins and receptor internalization into endosomes. Unlike canonical GPCR signaling, the β-arrestin association with the V_2R does not terminate $G\alpha_s$ activation, and thus, $G\alpha_s$-mediated signaling is sustained while the receptor is internalized. Here, we demonstrate that this V_2R ability to co-interact with G protein/β-arrestin and promote endosomal G protein signaling is not restricted to $G\alpha_s$, but also involves $G\alpha_{q/11}$. Furthermore, our data implies that β-arrestins potentiate $G\alpha_s/G\alpha_{q/11}$ activation at endosomes rather than terminating their signaling. Surprisingly, we found that the V_2R internalizes and promote endosomal G protein activation independent of β-arrestins to a minor degree. These new observations challenge the current model of endosomal GPCR signaling and suggest that this event can occur in both β-arrestin-dependent and -independent manners.

IMPACT STATEMENT

The vasopressin type 2 receptor promotes dual $G\alpha_s$ and $G\alpha_{q/11}$ signaling at early endosomes in β-arrestin-dependent and -independent manners.

INTRODUCTION

The vasopressin type 2 receptor (V_2R) is mainly known for its antidiuretic action in the kidney. Here, in the principal cells of the collecting duct, the V_2R regulates water reabsorption from pre-urine by promoting translocation of water channel aquaporin 2 (AQP2) located in intracellular vesicles to the apical membrane (Nielsen et al., 1993). The net result of this translocation is an enhanced water permeability. Defective V_2R signaling due to loss or gain of function mutations is associated with nephrogenic diabetes insipidus (Bichet & Bockenhauer, 2016) or nephrogenic syndrome of inappropriate antidiuresis (Carpentier et al., 2012), respectively.

The V_2R belongs to the superfamily of G protein-coupled receptors (GPCRs), membrane proteins that control almost all physiological processes. Canonically, stimulation of GPCRs leads to coupling to and activation of heterotrimeric G proteins ($G\alpha\beta\gamma$), which initiates downstream signaling cascades that control global cellular responses. GPCRs can couple to four main families of Gα protein isoforms: $G\alpha_{s/olf}$, $G\alpha_{i/o}$, $G\alpha_{q/11}$, and $G\alpha_{12/13}$. Activation of each family leads to distinct downstream signaling events and cell biological outcomes. G protein activation is usually short lived and followed by receptor phosphorylation by GPCR kinases, which drives the recruitment of β-arrestins (βarrs) to the phosphorylated receptor. As βarrs interact with the same region of the receptor as G proteins, their recruitment physically uncouples G proteins from the receptor which causes desensitization of G protein signaling (Pippig et al., 1993). In addition, βarrs scaffold several proteins involved in

endocytosis, which promotes receptor internalization into endosomes (Krupnick et al., 1997; Laporte et al., 1999).

Surprisingly, recent findings facilitated by the emergence of new molecular tools to interrogate signaling events with a subcellular resolution have challenged this plasma membrane centric view of G protein signaling. Several GPCRs, including the V_2R, have been reported to engage in G protein signaling after βarr-mediated receptor internalization into early endosomes and/or other intracellular compartments (Feinstein et al., 2013; Thomsen et al., 2016). This endosomal stimulation of G protein signaling by βarr-bound GPCRs has been difficult to reconcile with the aforementioned canonical understanding of GPCR signaling since G protein and βarr interactions with a single receptor were thought to be mutually exclusive. However, we discovered and delineated a new signaling paradigm whereby some GPCRs, including the V_2R, bind βarrs in a specific manner; in this conformation, also called the 'tail' conformation, βarr only interacts with the phosphorylated receptor carboxy-terminal tail while the transmembrane core of the receptor remains unoccupied (Cahill et al., 2017; Shukla et al., 2014). Interestingly, βarr in this tail conformation can promote certain βarr-mediated functions such as receptor internalization and signaling (Cahill et al., 2017; Kumari et al., 2016; Kumari et al., 2017). However, as βarr does not compete for the receptor G protein-binding site in this tail conformation, it does not desensitize G protein signaling (Cahill et al., 2017). Rather, the receptor in this conformation may interact simultaneously with G proteins and βarr to form a GPCR–G protein–βarr "megaplex" (Cahill et al., 2017; Nguyen et al., 2019; Thomsen et al., 2016). Thus, the simultaneous engagement with G protein and βarr allows the receptor in these megaplexes to maintain its ability to activate G protein signaling, even while being internalized into endosomes by βarrs. Noteworthy, endosomal $G\alpha_s$ signaling by V_2R has been associated with enhanced and sustained translocation of AQP2 to the plasma membrane to facilitate water reabsorption, and therefore, appears to play an important physiological role (Feinstein et al., 2013).

Although known as a $G\alpha_s$-coupled receptor, several studies report activation of the $G\alpha_{q/11}$ isoforms by V_2R (Avet et al., 2022; Heydenreich et al., 2022; Lykke et al., 2015; Zhu et al., 1994) as well as unproductive coupling to $G\alpha_{12}$ (Okashah et al., 2020). Therefore, we hypothesized that the V_2R form megaplexes with both $G\alpha_s$ and $G\alpha_{q/11}$ leading to endosomal activation of both $G\alpha_s$ and $G\alpha_{q/11}$. In addition, pulse-stimulation experiments of the V_2R and parathyroid hormone type 1 receptor (PTHR) demonstrated that sustained $G\alpha_s$-mediated signaling was enhanced by βarr (Feinstein et al., 2011; Feinstein et al., 2013). To address whether such βarr-mediated increase in G protein signaling is a result of direct coupling and activation of G proteins at endosomes, we here applied a combination of approaches based on engineered mini G proteins (mG proteins) (Nehme et al., 2017; Wan et al., 2018), enhanced bystander bioluminescence resonance energy transfer (EbBRET) (Namkung et al., 2016), nanoluciferase binary technology (NanoBiT) (Dixon et al., 2016), and confocal microscopy imaging.

RESULTS

The V_2R activates $G\alpha_s$ and $G\alpha_q$ from early endosomes

To measure the activation of the four families of G protein isoforms at the plasma membrane and early endosomes by the V_2R in real-time, we used mG proteins. The mG proteins are homogenously distributed in the cytosol under basal condition but translocate to the subcellular location of GPCRs upon stimulation (Carpenter & Tate, 2016; Nehme et al., 2017; Wan et al., 2018). In addition, we applied an EbBRET approach instead of a conventional BRET-based assay to monitor mG protein trafficking. EbBRET displays superior robustness and sensitivity, as well as higher dynamic spectrometric energy transfer signals associated to EbBRET as compared to conventional BRET, which is why this approach was favored (Namkung et al., 2016). We fused mG proteins to the luciferase from *Renilla reniformis* (Rluc) and anchored green fluorescent protein from the same species (rGFP) to the polybasic sequence and prenylation CAAX box of KRas (rGFP-CAAX), which is located at the plasma membrane (Zacharias et al., 2002), or to the early endosome marker Rab5 (Gorvel et al., 1991) (Figure 1A,B left panels). Four variants of mG proteins (mGs, mGsi, mGsq, and mG12) have been designed and shown to maintain the receptor-Gα protein specificity of the four Gα

subunit isoform families (Wan et al., 2018). In HEK293 cells expressing rGFP-CAAX, V_2R, and similar levels of Rluc-fused mG proteins (Figure 1-figure supplement 1A), arginine vasopressin (AVP) treatment induced a rapid recruitment of mGs and mGsq but not mGsi nor mG12 to the plasma membrane. Maximal recruitment of the mGs and mGsq were reached ~10 minutes after initial stimulation (Figure 1A right panel). These results suggest that the V_2R activates both $G\alpha_s$ and $G\alpha_{q/11}$ at the plasma membrane. In addition, AVP stimulation led to the recruitment of the same mG protein isoforms to early endosomes in cells expressing rGFP-Rab5, V_2R, and similar levels of Rluc-fused mG proteins (Figure 1B right panel, Figure 1-figure supplement 1B). In contrast to the plasma membrane response, mGs and mGsq recruitment to early endosomes were slower and reached maximal levels 45-60 minutes after initial stimulation with AVP (Figure 1B right panel).

Activation of $G\alpha_{q/11}$ canonically stimulates phospholipase Cβ (PLCβ), an enzyme that hydrolyzes membrane phosphoinositides into diacylglycerol (DAG) and inositol phosphate. Consequently, to validate $G\alpha_{q/11}$ activation at plasma membrane and early endosomes by the V_2R, we monitored the AVP-mediated production of DAG at these subcellular compartments. To monitor DAG at the plasma membrane, we used the C1b DAG-binding domain of PKCδ fused to Rluc (Rluc-C1b) and measured the EbBRET between Rluc-C1b and rGFP-CAAX (Wright et al., 2021) upon stimulation with AVP or vehicle (Figure 1C left panel). In line with the recruitment of mGsq at the plasma membrane observed in Figure 1A, AVP induced a recruitment of Rluc-C1b at the plasma membrane depicted by an increase of EbBRET values, which confirms the production of DAG at the plasma membrane by V_2R (Figure 1C right panel). Importantly, this production of DAG is $G\alpha_{q/11}$-dependent as a pre-treatment with YM254890, an inhibitor of $G\alpha_{q/11}$, abrogated this downstream response (Taniguchi et al., 2003). To measure the production of DAG at early endosomes by V_2R, we monitored the EbBRET between Rluc-C1b and rGFP-Rab5 upon V_2R stimulation (Figure 1D left panel). Similar to the observed recruitment of mGsq to the early endosomes (Figure 1B), AVP also induced a recruitment of Rluc-C1b to the early endosomal marker rGFP-Rab5, which suggests that DAG is produced at endosomal membranes (Figure 1D right panel). This endosomal DAG production was also inhibited by YM254890 treatment, which demonstrates that it is $G\alpha_{q/11}$-dependent (Figure 1D right panel). As DAG is an activator of protein kinase C (PKC), we further monitored PKC activation upon stimulation with AVP or vehicle. To measure PKC activation, we used an unimolecular BRET-based sensor composed of two Rluc-C1b-fused PKC consensus sequences (TLKI;pPKC1 and TLKD;pPKC2) that are connected to the phosphothreonine-binding domains FHA1 and FHA2 and the BRET acceptor GFP10 via a flexible linker (Namkung et al., 2018) (Figure 1E left panel). Upon phosphorylation of pPKC1 and pPKC2, FHA1 and FHA2 bind to these phosphorylated sequences resulting in an increased proximity between Rluc and GFP10 and a corresponding increase of BRET signal. In line with the AVP-mediated production of DAG, AVP treatment also induced phosphorylation of PKC in a $G\alpha_{q/11}$-dependent fashion (Figure 1E right panel).

To visualize V_2R-mediated activation of $G\alpha_s$ and $G\alpha_{q/11}$ at the plasma membrane and early endosomes we used confocal microscopy. For this purpose, we transfected HEK293 cells with mGs, mGsq, or mGsi (as negative control) fused to a HaloTag (Halo-mGs, Halo-mGsq, Halo-mGsi) along with the respective red fluorescent protein (RFP)-fused plasma membrane or early endosomes markers Lck (Ley et al., 1994) or early endosome antigen 1 (EEA1) (Simonsen et al., 1998). Upon HaloTag labeling with a fluorescent green ligand, mGs, mGsq, and mGsi were visible and homogenously distributed in the cytosol under basal condition (vehicle) (Figure 2A upper panels). In contrast, in cells treated with AVP for 10 minutes, mGs and mGsq but not mGsi were redistributed along the periphery of the cells where they colocalized with Lck (Figure 2A bottom panels, Figure 2B). These observations confirm that $G\alpha_s$ and $G\alpha_{q/11}$ are activated by the V_2R at the plasma membrane. In cells expressing the early endosomal marker EEA1, robust colocalization between the Halo-mG proteins and RFP-EEA1 were found 45 minutes after initial AVP-stimulation but not by vehicle treatment (Figure 2C,D). Together our EbBRET and confocal microscopy imaging data suggest that $G\alpha_s$ and $G\alpha_{q/11}$ are activated by V_2R first at plasma membrane, and later on, from early endosomes after the V_2R has been internalized.

The V_2R recruits $G\alpha_s$/$G\alpha_q$ and βarrs simultaneously

G protein activation from endosomes by some GPCRs is associated with the ability of the receptor to recruit G protein and βarr simultaneously to form a GPCR-βarr-G protein megaplex. As we already previously demonstrated that the V_2R forms V_2R-βarr-G_s megaplexes upon AVP stimulation (Thomsen et al., 2016), we here explored whether formation of such complexes potentially can be formed with $G_{q/11}$ as well. In addition to the V_2R, we also applied a chimeric V_2R harboring the carboxy-terminal tail of the β_2-adrenergic receptor (β_2AR) referred to as $V_2\beta_2AR$. We previously showed that the phosphorylated V_2R carboxy-tail forms stable complexes with βarr, a requirement of megaplex formation, whereas the carboxy-tail of the β_2AR does not (Cahill et al., 2017). Therefore, we expected that only the V_2R, but not the $V_2\beta_2AR$, recruits G proteins and βarrs simultaneously upon agonist challenge.

Both the V_2R and $V_2\beta_2AR$ bind to AVP with similar affinities and activate adenylyl cyclase via $G\alpha_s$ with similar potencies (Oakley et al., 1999). We monitored activation of the four Gα protein families at the plasma membrane by the $V_2\beta_2AR$ upon AVP treatment using the same approach utilized in Figure 1A. Similarly to the V_2R, the $V_2\beta_2AR$ activated both $G\alpha_s$ and $G\alpha_q$, but not $G\alpha_i$ nor $G\alpha_{12}$, at plasma membrane with a maximal response reached after ~10 minutes of stimulation (Figure 3A, Figure 3-figure supplement 1). While the V_2R and $V_2\beta_2AR$ are both reported to internalize via a βarr-dependent mechanism, βarr has been reported to rapidly dissociate from the $V_2\beta_2AR$ shortly after its recruitment to the plasma membrane due to its low affinity for this receptor chimera (Oakley et al., 1999). In contrast, βarr stays associated with the V_2R during its internalization into endosomes owning to its high affinity for the V_2R (Oakley et al., 1999). Here, we compared the kinetics of βarr1 and βarr2 recruitment to the V_2R and $V_2\beta_2AR$ at the plasma membrane and early endosomes by monitoring AVP-promoted EbBRET between Rluc-fused βarrs and rGFP-CAAX or rGFP-Rab5, respectively (Figure 3B left panel). At similar levels of receptor and βarr expressions (Figure 3-figure supplement 2), both receptors recruited βarr1 and βarr2 at plasma membrane maximally after 10 minutes of stimulation with AVP (Figure 3B right upper panel). However, the presence of βarrs at the plasma membrane declined rapidly hereafter 10 minutes in V_2R-expressing cells, while remaining for longer periods of time in $V_2\beta_2AR$-expressing cells. These findings are in line with the previous reported observations (Oakley et al., 1999). Additionally, the translocation of βarrs to the plasma membrane was more robust for the V_2R as compared to the $V_2\beta_2AR$, which is reminiscent from the higher affinity of βarrs for the V_2R as compared to the β_2AR (Oakley et al., 2000). In contrast to the rapid translocation of βarrs to the plasma membrane, AVP treatment induced a robust but slower enrichment of βarrs to early endosomes with V_2R reaching a maximal response after approximately 45 minutes of stimulation (Figure 3B right bottom panel). Importantly, as opposed to V_2R, AVP stimulation of $V_2\beta_2AR$ did not result in βarr translocation to early endosomes (Figure 3B right bottom panel). Consequently, the $V_2\beta_2AR$ represents a valuable negative control to investigate the ability to recruit G proteins and βarrs simultaneously at endosomes.

To track the simultaneous coupling of G proteins and βarrs to GPCRs in real-time, a nanoBiT approach was used. Both mGs and mGsq were fused to the large portion of nanoluciferase (large-BiT; LgBiT) and βarr1 to an optimized small peptide BiT (small BiT; SmBiT). Reconstitution of the complete and functional nanoluciferase, which catalyzes the conversion of coelenterazine h, results in emission of a bright luminescence signal. In our setup, close proximity of LgBiT and SmBiT only occurs when LgBiT-mG and SmBiT-βarr1 are recruited simultaneously to the receptor, which is a hallmark of megaplex formation (Figure 3C left panel). Using this approach, we detected bright luminescence signals involving mGs/βarr1 (Figure 3C upper right panel) and mGsq/βarr1 (Figure 3C bottom right panel) upon stimulation of the V_2R but not the $V_2\beta_2AR$. Interestingly, the dual coupling of $G\alpha_{q/11}$/βarr to V_2R appeared to be faster than the co-coupling of $G\alpha_s$/βarr. While 20 minutes was required to reach the maximal response of V_2R-stimulated mGs/βarr1 co-coupling, 8 minutes was sufficient to obtain the maximal levels of mGsq/βarr1 recruitment to the V_2R (Figure 3C right panels).

To visualize the simultaneous recruitment of G proteins and βarr to the receptors by confocal microscopy, we transfected HEK293 cells with βarr2 fused to strawberry (strawberry-βarr2), Halo-mGs or Halo-mGsq, and the V_2R or $V_2\beta_2AR$. In vehicle-treated cells, both mGs and βarr2 were homogenously distributed in the cytosol (Figure 3D upper panels). However, after prolonged

stimulation of V_2R with AVP, around 75% of βarr2 colocalized with mGs in endocytic vesicles (Figure 3D,F). In $V_2\beta_2AR$-stimulated cells, little to no colocalization was observed between βarr2 and mGs upon prolonged stimulation with AVP (Figure 3D,F). Surprisingly, however, some clusters of intracellular mGs were visible despite the absence of βarr2 (Figure 3D). As opposed to V_2R-expressing cells for which nearly all the clusters of intracellular mGs colocalize with βarr2, in $V_2\beta_2AR$-expressing cells around 75% of the intracellular mGs clusters do not colocalize with βarr2 (Figure 3G). These results suggest simultaneous coupling of $G\alpha_s$/βarr2 to the V_2R in endosomes but not to the $V_2\beta_2AR$. It is important to specify here that as mG proteins are recruited to receptors in the active conformation, the mG clusters are located where the active receptors are. Consequently, colocalization of mGs with βarr2 necessarily implies the presence of the active receptor in close proximity to both mGs and βarr2. In cells expressing mGsq, both mGsq and βarr2 were also homogenously distributed in the cytosol when cells were treated with the vehicle (Figure 3E upper panels). Upon AVP stimulation, approximately 75% of βarr2 colocalized with mGsq in intracellular vesicles in V_2R-expressing cells, whereas poor colocalization was observed in $V_2\beta_2AR$-expressing cells (Figure 3E,F). Similarly to cells expressing mGs, clear clusters of intracellular mGsq were visible in cells expressing $V_2\beta_2AR$ (Figure 3E,G), suggesting a certain level of endosomal $G\alpha_s$/$G\alpha_q$ signaling despite the absence of βarr2.

βarr-dependent and -independent endosomal G protein activation by the V_2R

Activation of $G\alpha_s$ and $G\alpha_{q/11}$ by the $V_2\beta_2AR$ from endosome-like structures in the absence of local βarrs raises the possibility that the V_2R can activate these G proteins from endosomes in both βarr-dependent and -independent manners. To test this hypothesis, we compared AVP-induced $G\alpha_s$ and $G\alpha_{q/11}$ activation at plasma membrane and endosomes in CRISPR/Cas9-engineered βarr1- and βarr2-deficient HEK293 cells (Δβarr1/2) (Namkung et al., 2016) as well as their parental cellular counterpart. The surface expression of V_2R was matched in both cellular backgrounds (Figure 4-figure supplement 1). Using the EbBRET biosensors described in Figure 1A-B, we performed AVP concentration-response characterization of $G\alpha_s$ and $G\alpha_{q/11}$ activation at the plasma membrane (Figure 4A) and early endosomes (Figure 4B) in parental and Δβarr1/2 HEK293 cells. In contrast to $G\alpha_s$ and $G\alpha_{q/11}$ activation at the plasma membrane, which were not negatively affected by the absence of βarrs (Figure 4A, Table 1), we observed a robust decrease in the ability of the V_2R to activate $G\alpha_s$ and $G\alpha_q$ at endosomes in Δβarr1/2 cells as compared to their parental counterpart (Figure 4B, Table 1). These data demonstrate the important role of βarrs in endosomal $G\alpha_s$/$G\alpha_{q/11}$ activation by the V_2R. However, although the Δβarr1/2 cells do not express βarrs, we still observed significant residual G protein activation from endosomes. This surprising observation suggests that the V_2R internalizes into endosomes to some extent in a βarr-independent manner from where G proteins are stimulated. To probe this possibility, we compared V_2R internalization in parental and Δβarr1/2 HEK293 cells expressing rGFP-CAAX and equivalent amounts of V_2R fused to Rluc at its carboxy-terminal tail (V_2R-Rluc) (Figure 3C left panel, Figure 4-figure supplement 2). In parental HEK293 cells, AVP-stimulation of the V_2R-Rluc led to a robust decrease of EbBRET values, which indicates strong receptor internalization (Figure 4C right panel). Interestingly, we also observed significant internalization of the V_2R in Δβarr1/2 HEK293 cells, although less than in the parental cells (Figure 4C right panel). These results suggest that a minor population of V_2R internalizes independently of βarrs and contributes to endosomal $G\alpha_s$ and $G\alpha_{q/11}$ signaling.

βarrs potentiate endosomal $G\alpha_s$ and $G\alpha_q$ activation by the V_2R.

Although our data suggest that a minor population of V_2R internalizes in the absence of βarrs and contribute to V_2R-mediated endosomal $G\alpha_s$ signaling, it has been reported that βarr binding to the V_2R and parathyroid hormone receptor (PTHR) potentiates endosomal $G\alpha_s$ signalling (Feinstein et al., 2011; Feinstein et al., 2013). To verify this and determine if this potentiator effect of βarrs also affects endosomal $G\alpha_{q/11}$ signaling, we compared endosomal $G\alpha_s$ and $G\alpha_{q/11}$ activation in cells expressing similar levels of V_2R or $V_2\beta_2AR$ (Figure 4-figure supplement 3). Our rationale for using these two receptors is that if βarrs potentiate endosomal G protein activation, this potentiator effect will be observed to a greater extent for the V_2R since this receptor associates more robustly with

βarrs as compared to the $V_2\beta_2$AR. Using the same biosensors as in Figure 1A-B, we performed AVP dose-response curves of mGs and mGsq recruitment to the plasma membrane and early endosomes (Figure 4-figure supplement 4, Table 2). From the dose-response curves obtained (Figure 4-figure supplement 4, Table 2), we determined the transduction coefficient log(τ/Ka), a parameter that combines efficiency and potency to determine the overall G protein transduction, for each condition using the operational model of Kenakin and Christopoulos (Kenakin et al., 2012). In cells expressing mGs, the transduction coefficients of $G\alpha_s$ activation at the plasma membrane were similar for the V_2R and $V_2\beta_2$AR, but higher for the V_2R than $V_2\beta_2$AR in early endosomes (Figure 4D left panel, Table 2). Similarly, in cells expressing mGsq, the transduction coefficients of $G\alpha_{q/11}$ activation at the plasma membrane were similar for the V_2R and $V_2\beta_2$AR, but higher for the V_2R than $V_2\beta_2$AR in early endosomes (Figure 4D right panel, Table 2). Altogether these results indicate that βarrs potentiate activation of G proteins by the V_2R in early endosomes.

DISCUSSION

In the present work, we addressed the spatial aspect of G protein signaling by the V_2R and investigated the potential role of βarrs in modulating these responses in HEK293 cells. Several studies report activation of $G\alpha_s$ and $G\alpha_{q/11}$ by the V_2R using a wide range of assays (Avet et al., 2022; Heydenreich et al., 2022; Inoue et al., 2019; Okashah et al., 2020; Zhu et al., 1994). However, these assays lack spatial resolution or are measured by default at the plasma membrane. Here, we demonstrated that both $G\alpha_s$ and $G\alpha_{q/11}$ are activated by the V_2R at the plasma membrane and early endosomes using a mG protein-based approach as well as biosensors of downstream signaling. The mG protein-based approach measures the receptor's ability to couple to G proteins in real-time rather than G protein-mediated signaling outputs. Whether G protein coupling to the V_2R follows similar kinetic patterns in primary cells expressing the receptor endogenously was not interrogated in this study. The PTHR, a GPCR that regulates mineral ion homeostasis and bone development, also couples to both $G\alpha_s$ and $G\alpha_{q/11}$ (Schwindinger et al., 1998). Similar to our observations of the V_2R, the reduction of PTHR internalization by βarr1 and βarr2 depletion strongly decreases endosomal $G\alpha_s$/cAMP signaling. However, in contrast to the V_2R, βarr-mediated receptor internalization shuts down $G\alpha_{q/11}$-mediated responses, and thus, the PTHR does not appear to stimulate $G\alpha_{q/11}$ from endosomes (Castro et al., 2002; Feinstein et al., 2011).

The reason for this inability of internalized PTHR to activate $G\alpha_{q/11}$ from endosomes is not known. However, it is unlikely to be a general feature of these G protein isoforms as multiple laboratories have reported endosomal GPCR signaling events downstream of $G\alpha_{q/11}$ activation activation (Gorvin et al., 2018; Jensen et al., 2017; Jimenez-Vargas et al., 2018). These events include measurements of signal-amplified responses such as protein kinase C (PKC) recruitment or ERK1/2 activation (Gorvin et al., 2018; Jensen et al., 2017; Jimenez-Vargas et al., 2018). Recently, direct activation of $G\alpha_{q/11}$ from early endosomes was monitored using a mG protein-based approach and effector membrane translocation assay (EMTA) (Wright et al., 2021). In this study, Wright *et al*. demonstrated that stimulation of $G\alpha_{q/11}$ protein isoforms by receptors at the plasma membrane does not necessarily lead to the activation of the exact same isoforms at endosomes. For example, the authors showed that the thromboxane A_2 alpha isoform receptor (TPαR) robustly activates all the $G\alpha_{q/11}$ isoforms ($G\alpha_q$, $G\alpha_{11}$, $G\alpha_{14}$, and $G\alpha_{15}$) at the plasma membrane, but only activates $G\alpha_q$ and $G\alpha_{11}$ isoforms at endosomes. In contrast, the muscarinic acetylcholine M_3 receptor (M_3R) activates all four $G\alpha_{q/11}$ isoforms both at plasma membrane and endosomes. While G protein selectivity at plasma membrane is mainly dependent on receptor conformation (Rose et al., 2014; Van Eps et al., 2018), specific residues present at the GPCR-Gα protein interface (Flock et al., 2017) as well as the location and duration of these intermolecular interactions (Sandhu et al., 2022), endosomal G protein activation seems to be controlled by additional factors that are not fully understood.

The presence of serine/threonine phosphorylation site clusters at the carboxy-terminal tail of GPCRs delineates two major classes of receptors; class A and class B (Oakley et al., 2000). Class A GPCRs such as the β_2AR are defined by harboring few single phosphorylation sites, which form interactions with positively charged residues of βarrs (Shukla et al., 2013). In addition to the phosphorylated receptor residues, the class A GPCR–βarr association also depends on an interaction between the

βarr fingerloop region and the receptor transmembrane core, which sterically block G protein access to the GPCR (Cahill et al., 2017; Shukla et al., 2014). The class A GPCR–βarr association is transient and the complex dissociates shortly after endocytosis, which results in receptor recycling back to the cell surface. In contrast, class B GPCRs including the V_2R are defined by having phosphorylation site clusters in the carboxy-terminal tail that form highly stable associations with βarrs solely through this region. This strong interaction leads to prolonged receptor internalization into endosomes (Cahill et al., 2017). As the stability of this GPCR–βarr complex 'tail' conformation does not depend on the interaction between the βarr fingerloop region and the receptor core, the GPCR can interact simultaneously with G proteins to forms a GPCR–G protein–βarr megaplex (Nguyen et al., 2019; Thomsen et al., 2016). As the receptors in these megaplexes maintain their ability to activate G proteins, they can internalize via βarrs into different intracellular compartments while stimulating G protein signaling for prolonged periods of time (Cahill et al., 2017; Calebiro et al., 2009; Feinstein et al., 2013; Ferrandon et al., 2009; Thomsen et al., 2016). Previously, formation of megaplexes at intracellular compartments has only been reported involving $G\alpha_s$ or $G\alpha_{i/o}$ proteins (Hyunggu Hahn, 2022; Smith et al., 2021; Thomsen et al., 2016). In the present study we demonstrate that megaplex formation is not confined to these G protein isoforms but also appears to form with other G protein isoforms such as $G\alpha_{q/11}$.

An interesting aspect of βarr/megaplex-dependent endosomal G protein signaling is whether βarrs only acts as a vehicle that transports GPCRs to this subcellular location from where they activate G proteins or whether βarrs in megaplexes themselves directly modulate G protein activity. In the current study, we show that βarrs directly potentiate G protein activation by the V_2R in early endosomes (Figure 4D). These findings are further supported by Feinstein *et al.* who previously demonstrated that V_2R-stimulated G protein activation is positively modulated by the presence of βarr2 (Feinstein et al., 2013). However, in the recent cryo-electron microscopy high-resolution structure of an engineered class B GPCR–Gs–βarr1 megaplex, no direct interaction between the heterotrimeric Gs and βarr1 was observed, and thus, it is not obvious how βarrs may affect G protein activity from this structure (Nguyen et al., 2019). On the other hand, biochemical studies of the megaplex and G protein–βarrs interactions demonstrated that βarr can serve as a scaffold for the Gβγ subunits that are released upon activation of the heterotrimeric G protein (Thomsen et al., 2016; Wehbi et al., 2013; Yang et al., 2009). Thus, this Gβγ scaffolding role of βarr may confine $G\alpha_s$ and $G\alpha_{q/11}$ near endosomally-located V_2R, leading to their re-activation as soon as the inactive GDP-bound Gα with Gβγ subunits reassemble. The results of such activation mechanism would be a net increase in the G protein activation rate.

In cells, confocal microscopy imaging and proximity assays such as BRET have been used to detect megaplex formation at class B GPCRs including the V_2R (Thomsen et al., 2016). However, these experimental approaches as well as other techniques that detect protein associations in intact cells cannot discriminate between direct protein–protein interactions and proteins that are in close proximity to each other yet not physically connected. Therefore, the exact protein configuration of detected megaplexes is extremely difficult to confirm in cells, and there is a theoretical possibility that the responses measured and interpreted as megaplexes formation may arise from receptor dimers where each individual receptor binds either G protein, βarr, or both at the same time. To confirm that a single receptor in cells can physically interact with G protein and βarr simultaneously, we previously conducted a series of experiments with class B GPCR–βarr fusions where the two proteins are covalently attached at the receptor carboxy-terminal tail. We showed that despite the GPCR–βarr coupling being fully functional and this fusion "complex" internalizing constitutively, the receptor maintains its ability to activate G proteins upon agonist stimulation (Nguyen et al., 2019; Thomsen et al., 2016). Thus, these results definitively showed that single receptor megaplexes can *physically* form in cells.

Surprisingly, our results using Δβarr1/2 cells indicate that the V_2R not only promote endosomal G protein signaling in a βarr/megaplex-dependent manner but also can internalize and activate G proteins from endosomes in a βarr-independent fashion (Figure 4B,C). Although our data showed that βarr-independent endosomal G protein activation is substantial less effective than the βarr-

dependent mechanism for the V_2R, it still represents an alternative mode of endosomal GPCR signaling that little is known about. For some receptors such as the apelin receptor βarr association is not required for clathrin-mediated internalization (Pope et al., 2016). Alternatively, several GPCRs also internalize independently of any clathrin and βarr associations via caveolae or by fast endophilin-mediated endocytosis (FEME) (Moo et al., 2021). Notably, the glucagon-like peptide-1 receptor (GLP1R) internalizes in a βarr-independent manner and signals via $G\alpha_s$ from endosomes to promote glucose-stimulated insulin secretion in pancreatic β-cells, which highlights the physiological relevance of βarr-independent endosomal G protein signaling (Claing et al., 2000; Kuna et al., 2013). Interestingly, in a very recent study of the vasoactive intestinal peptide receptor 1 (VIPR1) by Blythe & von Zastrow, it was shown that VIPR1 promotes robust G protein signaling from endosomes and that this occurs in a completely βarr-independent fashion (Blythe, 2023). Surprisingly, the authors observed that agonist-stimulation of VIPR1 led to recruitment of βarr1 and receptor internalization into endosomes where VIPR1 and βarr1 colocalized. However, despite this potential interaction between VIPR1 and βarrs, the presence of βarr1/2 had little to no effect on receptor internalization and the ability of VIPR1 to activate G protein from endosomes (Blythe, 2023). As three independent studies using two different receptor systems now have found that endosomal G protein signaling can be achieved independent of βarrs, it is likely that this alternative mode of signaling represents a more general mechanism that is utilized by multiple GPCRs to regulate important physiological functions. Thus, further investigation into the details of βarr-independent receptor internalization and endosomal G protein signaling is much needed.

In summary, in the present study we gain new insights into how internalized V_2R stimulates G protein signaling from endosomes, which require us to modify the current model (Figure 5). We demonstrated that V_2R-mediated endosomal G protein activation is not restricted to the $G\alpha_s$ isoform but also occurs with the $G\alpha_{q/11}$ isoforms. A major part of this endosomal G protein activation is βarr-dependent, and presumably takes place through the formation of V_2R–G protein–βarr megaplexes. Interestingly, the presence of βarrs in these megaplexes potentiates the ability of the V_2R to activate G protein within endosomes. Surprisingly, we found that this mechanism is not the only way internalized V_2R stimulates G protein signaling from endosomes since this event can take place in a completely βarr-independent fashion as well. The underlying details of how βarr-independent endosomal G protein activation by the V_2R takes place is not known. However, since similar observations were made of other GPCRs including the GLP1R and VIPR1, the mechanism might represent a general aspect of GPCR biology that control important physiological and pathophysiological processes.

MATERIALS AND METHODS

Cell culture and transfection

HEK293 clonal cell line (HEK293SL cells) and referred as HEK293 cells as well as the HEK293 cells devoid of βarr1 and βarr2 referred as Δβarr1/2 cells were a gift from Stephane Laporte (McGill University, Montreal, Quebec, Canada) and previously described (Namkung et al., 2016). These cells were cultured in Dulbecco's Modified Eagle's Medium (DMEM) high glucose (Life Technologies, Paisley, UK) supplemented with 10% fetal bovine serum and 100 units per ml penicillin-streptomycin (Life Technologies, Paisley, UK), maintained at 37°C and 5% CO_2 and passaged every 3-4 days using trypsin-EDTA 0.05% (Life Technologies, Paisley, UK) to detach the cells. DNA to be transfected was combined with salmon sperm DNA (Thermo Fisher Scientific, Cambridge, UK) to obtain a total of 1 µg DNA per condition. Linear polyethyleneimine 25K (PEI; Polysciences Europe GmbH, Germany) was combined with DNA (3 µg PEI per µg of DNA), vortexed and incubated 20 minutes before adding a cell suspension containing 300,000 cells per ml (1.2 ml of cells per condition). The appropriate volume of cells containing the DNA was seeded and cells were incubated for 48 hours before assay.

DNA plasmids

All DNA constructs were cloned into pcDNA3.1(+) expression plasmid except if stated otherwise. V_2R and $V_2\beta_2AR$ were tagged with a HA epitope in amino-terminal of the receptors. HA-V_2R was synthetized by GenScript and HA-$V_2\beta_2AR$ was generously provided by Dr Robert Lefkowitz (Duke

University, USA). C-tRFP-Lck (cloned into PCMV6-AC-RFP expression vector) and TagRFP-T-EEA1 (cloned into pEGFP-C1 vector) were purchased from Addgene (respectively #RC100049 and #42635). Strawberry-βarr2 was a gift from Prof. Marc G. Caron (Duke University, USA). rGFP-CAAX (Namkung et al., 2016), rGFP-Rab5 (Namkung et al., 2016), V_2R-Rluc (Namkung et al., 2016), Rluc-βarr1 (Zimmerman et al., 2012), Rluc-βarr2 (Quoyer et al., 2013), Rluc-C1b (Wright et al., 2021), and the BRET-based unimolecular PKC sensor (Namkung et al., 2018) were previously described. Rluc-mGs, Rluc-mGsi, Rluc-mGsq, and Rluc-mG12 were synthetized by Twist Bioscience and cloned into pTwistCMV expression vector. The Venus tag in NES-Venus-mGs, NES-Venus-mGsi, NES-Venus-mGsq, and NES-Venus-mG12 previously described (Wan et al., 2018) was replaced by Rluc. Halo-tagged mG constructs was kindly provided by Prof. Nevin A. Lambert (Augusta University, USA). LgBiT-mGsq and SmBiT-βarr1 were synthetized by GenScript. mGsq and βarr1 were tagged in amino-terminal with LgBiT and a linker peptide and SmBiT, respectively.

Bioluminescence Resonance Energy Transfer (BRET) assays

The cell suspension containing DNA (BRET/EbBRET biosensors and receptors) were seeded in white 96-well plates (Greiner, Stonehouse, UK) at 30,000 cells/well (100 μl per well). 48 hours after transfection, cells were washed with DPBS (Life Technologies, Paisley, UK) and assayed in Tyrode's buffer containing 137 mM NaCl, 0.9 mM KCl, 1 mM $MgCl_2$, 11.9 mM $NaHCO_3$, 3.6 mM NaH_2PO_4, 25 mM Hepes, 5.5 mM glucose, 1 mM $CaCl_2$ (pH 7.4) at 37°C. AVP or vehicle (water) were added and cells incubated at 37°C for the required time. 5 minutes before reading, 2.5 μM of the Rluc substrate coelenterazine 400a (NanoLight Technology, Pinetop, AZ, USA) was added, respectively. All BRET and EbBRET measurements were performed using a FLUOstar Omega microplate reader (BMG Labtech, Ortenberg, Germany) with an acceptor filter (515 ± 30 nm) and donor filter (410 ± 80 nm). BRET/EbBRET values were determined by calculating the ratio of the light intensity emitted by the acceptor over the light intensity emitted by the donor. ΔEbBRET is defined as the values of EbBRET in presence of AVP (Merck Life Science, Gillingham, UK) minus the value obtained with vehicle. Dose-response curves were fitted using nonlinear regression using a 4-parameter equation and the basal ΔEbBRET was fixed to zero. Statistical significance of parameters of dose-response curves (AVP-induced maximal efficacy or potency) was established by comparing independent fits with a global fit that shares the selected parameter using extra sum-of-squares F test. The transduction coefficients Log(τ/Ka) were determined using the operational from Kenakin and Christopoulos as previously described (van der Westhuizen et al., 2014).

NanoBiT assay

The nanoBiT assay to measure proximity between LgBiT-mG proteins and SmBiT-βarr1 has been reported previously (Hahn et al., 2022). In short, 2,000,000 cells were seeded per well in 6 well plates. 24 hours later, 125 ng SmBiT-βarr1, 1000 ng V_2R or $V_2\beta_2$AR, and 125 ng LgBiT-mGs or 1000 ng LgBiT-mGsq were transfected into the cells using Lipofectamine 3000 transfection reagent (Thermo Fisher Scientific, Waltham, MA, USA). The next day, transfected cells were detached and 100,000 cells/well were plated into a Poly-D-lysine-coated white 96-well Microplate (Corning, Corning, NY, USA) and incubated overnight at 37°C. The cells were equilibrated in Opti-MEM (Life Technologies, Paisley, UK) at 37°C for 60 minutes. Coelenterazine-h (NanoLight Technology, Pinetop, AZ, USA) was added at a final concentration of 10 μM before starting the measurement. After establishing a baseline response for 2 minutes, cells were stimulated with AVP added at a final concentration of 100 nM and the luminescence was measured for additional 20 minutes. The signal was detected at 550 nm using a PHERAstar *FSX* instrument (BMG LabTech, Cary, NC, USA). ΔRLU is defined as the values of relative luminescence in presence of AVP minus the value obtained with vehicle.

Confocal microscopy

Cells containing plasmid DNA encoding for fluorescent-tagged localization markers or strawberry-βarr2, receptors, and mGs, mGsq, or mGsi fused to HaloTag were seeded in 8-well glass chambered slides (Thistle Scientific, Uddingston, Glasgow, UK) at 30,000 cells per well. The day of the assay, mG constructs were labelled by adding HaloTag® Oregon Green® Ligand (Promega, Chilworth, UK) to cells at a final concentration of 1 μM in the culture media and incubated 15 minutes (37°C, 5% CO_2). Cells were washed 3 times with the media and incubated 30 minutes (37°C, 5% CO_2) for the

last wash. The media was aspirated, replaced by Tyrode's buffer and cells were stimulated with AVP or vehicle (water) for the required time at 37°C, 5% CO_2. At the end of the incubation, the media was aspirated and cells were fixed by adding 300 μl per well of 4% paraformaldehyde in PBS (Life Technologies, Paisley, UK) and incubated at room temperature for 10 minutes. The paraformaldehyde solution was aspirated, replaced by DPBS and cells were incubated for 10 minutes before being replaced by Tyrode's buffer (300 μl per well) and visualized on a SP8 confocal microscope (Leica Biosystems, Nussloch, Germany) at 63X magnification. Images were quantified using Imaris cell imaging software version 9.9.1 (Oxford Instruments, Abingdon, UK). For each image, a threshold for the red channel was established by selecting the lower intensity from the region of interest (plasma membrane, endosomes, or βarr2). The percentage of colocalization was determined by the percentage of the material from the red channel above threshold colocalized with the material from the green channel. To quantify the percentage of colocalization for confocal microscopy images, the "surfaces" module was selected isolating cells containing the region of interest for each image. Thresholds for each channel were established by selecting the lower intensity from the region of interest (plasma membrane, endosomes, or βarr2). Data are reported as red volume (red voxels) above the threshold that is co-localized with green volume (green voxels) above the threshold and reported as percentage.

ELISA

To measure the relative cell surface expression of V_2R and $V_2\beta_2AR$ (both tagged with a HA epitope at their amino-terminal), the same cell suspension containing DNA that was used for EbBRET assays was seeded in white 96-well plates previously coated with Poly-D-lysine (Bio-Techne, Abingdon, UK) at 30,000 cells/well (100 μl per well). Non transfected cells were used to establish the background of the assay. For the coating, the Poly-D-Lysine solution (0.1 mg per ml) was added (50 μl per well) and the plates incubated at 37 °C for at least 30 minutes. Following the incubation, the solution was aspirated and wells washed two times with DPBS before adding the cell suspension containing DNA. 48 hours after seeding, cells were washed with DPBS and fixed by adding 50 μl per well of 4% paraformaldehyde in PBS and incubated at room temperature for 10 minutes. The fixing solution was aspirated and wells washed 3 times in a washing buffer composed of DPBS containing 0.5% of BSA (Merck Life Science, Gillingham, UK). The washing buffer was left in the wells for 10 minutes following the last wash. After the 10 minute incubation, the buffer was removed and 50 μl per well of monoclonal 3F10 anti-HA-Peroxidase (Merck Life Science, Gillingham, UK) 12.5 ng per ml in washing buffer was added and the plate incubated 1 hour at room temperature. The antibody was aspirated and wells washed 3 times with the washing buffer. The washing buffer was left in the wells for 10 minutes following the last wash and wells were washed again 3 times with DBPS only. After aspiration of the DPBS, 100 μl per well of SigmaFast™ OPD (Merck Life Science, Gillingham, UK) solution prepared as recommended by the manufacturer was added. Wells were incubated in presence of the OPD solution until the wells containing cells expressing receptors become yellow (typically 10 minutes). The reaction was stopped by addition of 25 μl per well of hydrochloride 3M in water. 100 μl per well were transferred to a transparent clear 96-well flat bottom plate (Thermo Fisher Scientific, Cambridge, UK) and absorbance at 492 nm was measured using a FLUOstar Omega microplate reader. The net absorbance represents the absorbance measured in presence of receptor minus the background (i.e. absorbance measured in absence of receptor).

Data processing and statistical analyses

In all experiments at least three independent experiments were performed and for each experiment. *n* value is provided in the corresponding figure legend. All experiments are performed in quadruplicates. A P value ≤ 0.05 was considered as statistically significant for all analyses. Normally distributed and normalized data to control for unwanted sources of variation are shown as mean ± standard error on mean (SEM). All statistical analyses and nonlinear regressions were performed using GraphPad Prism 9.4.1 software.

FUNDING INFORMATION

This work was supported by a Wellcome Trust Seed Award (215229/Z/19/Z) and a New Investigator Award from the UKRI Biotechnology and Biological Sciences Research Council (BB/X002578/1) to

BP, a research grant from the LEO Foundation (LF18043) and the NIH (1R35GM147088 and 1R21CA243052) to ARBT, a Doctoral Studentship from the Department for the Economy (DfE) Northern Ireland to CD, a Fellowship from the Armagh Tigers Charitable Trust to AW, and a CITI-GENS Horizon2020 Marie Sklodowska-Curie Doctoral Scholarship to AAG.

ACKNOWLEDGEMENTS

We would like to thank Stéphane Laporte for providing the parental and CRISPR/Cas9-engineered β-arrestin1/2-deficient HEK293 cells, Michel Bouvier for providing the rGFP-CAAX and rGFP-Rab5 EbBRET biosensors as well as the BRET-based PKC sensor.

REFERENCES

Avet, C., Mancini, A., Breton, B., Le Gouill, C., Hauser, A. S., Normand, C., . . . Bouvier, M. (2022). Effector membrane translocation biosensors reveal G protein and betaarrestin coupling profiles of 100 therapeutically relevant GPCRs. *Elife*, *11*. https://doi.org/10.7554/eLife.74101

Bichet, D. G., & Bockenhauer, D. (2016). Genetic forms of nephrogenic diabetes insipidus (NDI): Vasopressin receptor defect (X-linked) and aquaporin defect (autosomal recessive and dominant). *Best Pract Res Clin Endocrinol Metab*, *30*(2), 263-276. https://doi.org/10.1016/j.beem.2016.02.010

Blythe, E. E. v. Z., M. (2023). β-arrestin-independent endosomal cAMP signaling by a polypeptide hormone GPCR. https://doi.org/https://doi.org/10.1101/2022.09.07.506997

Cahill, T. J., 3rd, Thomsen, A. R., Tarrasch, J. T., Plouffe, B., Nguyen, A. H., Yang, F., . . . Lefkowitz, R. J. (2017). Distinct conformations of GPCR-beta-arrestin complexes mediate desensitization, signaling, and endocytosis. *Proc Natl Acad Sci U S A*, *114*(10), 2562-2567. https://doi.org/10.1073/pnas.1701529114

Calebiro, D., Nikolaev, V. O., Gagliani, M. C., de Filippis, T., Dees, C., Tacchetti, C., . . . Lohse, M. J. (2009). Persistent cAMP-signals triggered by internalized G-protein-coupled receptors. *PLoS Biol*, *7*(8), e1000172. https://doi.org/10.1371/journal.pbio.1000172

Carpenter, B., & Tate, C. G. (2016). Engineering a minimal G protein to facilitate crystallisation of G protein-coupled receptors in their active conformation. *Protein Eng Des Sel*, *29*(12), 583-594. https://doi.org/10.1093/protein/gzw049

Carpentier, E., Greenbaum, L. A., Rochdi, D., Abrol, R., Goddard, W. A., 3rd, Bichet, D. G., & Bouvier, M. (2012). Identification and characterization of an activating F229V substitution in the V2 vasopressin receptor in an infant with NSIAD. *J Am Soc Nephrol*, *23*(10), 1635-1640. https://doi.org/10.1681/ASN.2012010077

Castro, M., Dicker, F., Vilardaga, J. P., Krasel, C., Bernhardt, M., & Lohse, M. J. (2002). Dual regulation of the parathyroid hormone (PTH)/PTH-related peptide receptor signaling by protein kinase C and beta-arrestins. *Endocrinology*, *143*(10), 3854-3865. https://doi.org/10.1210/en.2002-220232

Claing, A., Perry, S. J., Achiriloaie, M., Walker, J. K., Albanesi, J. P., Lefkowitz, R. J., & Premont, R. T. (2000). Multiple endocytic pathways of G protein-coupled receptors delineated by GIT1 sensitivity. *Proc Natl Acad Sci U S A*, *97*(3), 1119-1124. https://doi.org/10.1073/pnas.97.3.1119

Dixon, A. S., Schwinn, M. K., Hall, M. P., Zimmerman, K., Otto, P., Lubben, T. H., . . . Wood, K. V. (2016). NanoLuc Complementation Reporter Optimized for Accurate Measurement of Protein Interactions in Cells. *ACS Chem Biol*, *11*(2), 400-408. https://doi.org/10.1021/acschembio.5b00753

Feinstein, T. N., Wehbi, V. L., Ardura, J. A., Wheeler, D. S., Ferrandon, S., Gardella, T. J., & Vilardaga, J. P. (2011). Retromer terminates the generation of cAMP by internalized PTH receptors. *Nat Chem Biol*, *7*(5), 278-284. https://doi.org/10.1038/nchembio.545

Feinstein, T. N., Yui, N., Webber, M. J., Wehbi, V. L., Stevenson, H. P., King, J. D., Jr., . . . Vilardaga, J. P. (2013). Noncanonical control of vasopressin receptor type 2 signaling by retromer and arrestin. *J Biol Chem*, *288*(39), 27849-27860. https://doi.org/10.1074/jbc.M112.445098

Ferrandon, S., Feinstein, T. N., Castro, M., Wang, B., Bouley, R., Potts, J. T., . . . Vilardaga, J. P. (2009). Sustained cyclic AMP production by parathyroid hormone receptor endocytosis. *Nat Chem Biol*, *5*(10), 734-742. https://doi.org/10.1038/nchembio.206

Flock, T., Hauser, A. S., Lund, N., Gloriam, D. E., Balaji, S., & Babu, M. M. (2017). Selectivity determinants of GPCR-G-protein binding. *Nature*, *545*(7654), 317-322. https://doi.org/10.1038/nature22070

Gorvel, J. P., Chavrier, P., Zerial, M., & Gruenberg, J. (1991). rab5 controls early endosome fusion in vitro. *Cell*, *64*(5), 915-925. https://doi.org/10.1016/0092-8674(91)90316-q

Gorvin, C. M., Rogers, A., Hastoy, B., Tarasov, A. I., Frost, M., Sposini, S., . . . Thakker, R. V. (2018). AP2sigma Mutations Impair Calcium-Sensing Receptor Trafficking and Signaling, and Show an Endosomal Pathway to Spatially Direct G-Protein Selectivity. *Cell Rep*, *22*(4), 1054-1066. https://doi.org/10.1016/j.celrep.2017.12.089

Hahn, H., Daly, C., IV, J. L., Perry-Hauser, N. A., Inoue, A., Plouffe, B., & Thomsen, A. R. B. (2022). Endosomal Chemokine Receptor Signalosomes Regulate Central Mechanisms Underlying Cell Migration. *BioRxiv*. https://doi.org/https://doi.org/10.1101/2022.09.27.509755

Heydenreich, F. M., Plouffe, B., Rizk, A., Milic, D., Zhou, J., Breton, B., . . . Veprintsev, D. (2022). Michaelis-Menten quantification of ligand signalling bias applied to the promiscuous Vasopressin V2 receptor. *Mol Pharmacol*. https://doi.org/10.1124/molpharm.122.000497

Hyunggu Hahn, C. D., John Little IV, Nicole A. Perry-Hauser, Asuka Inoue, Bianca Plouffe, Alex R.B. Thomsen. (2022). Endosomal Chemokine Receptor Signalosomes Regulate Central Mechanisms Underlying Cell Migration. https://doi.org/https://doi.org/10.1101/2022.09.27.509755

Inoue, A., Raimondi, F., Kadji, F. M. N., Singh, G., Kishi, T., Uwamizu, A., . . . Russell, R. B. (2019). Illuminating G-Protein-Coupling Selectivity of GPCRs. *Cell*, *177*(7), 1933-1947 e1925. https://doi.org/10.1016/j.cell.2019.04.044

Jensen, D. D., Lieu, T., Halls, M. L., Veldhuis, N. A., Imlach, W. L., Mai, Q. N., . . . Bunnett, N. W. (2017). Neurokinin 1 receptor signaling in endosomes mediates sustained nociception and is a viable therapeutic target for prolonged pain relief. *Sci Transl Med*, *9*(392). https://doi.org/10.1126/scitranslmed.aal3447

Jimenez-Vargas, N. N., Pattison, L. A., Zhao, P., Lieu, T., Latorre, R., Jensen, D. D., . . . Bunnett, N. W. (2018). Protease-activated receptor-2 in endosomes signals persistent pain of irritable bowel syndrome. *Proc Natl Acad Sci U S A*, *115*(31), E7438-E7447. https://doi.org/10.1073/pnas.1721891115

Kenakin, T., Watson, C., Muniz-Medina, V., Christopoulos, A., & Novick, S. (2012). A simple method for quantifying functional selectivity and agonist bias. *ACS Chem Neurosci*, *3*(3), 193-203. https://doi.org/10.1021/cn200111m

Krupnick, J. G., Goodman, O. B., Jr., Keen, J. H., & Benovic, J. L. (1997). Arrestin/clathrin interaction. Localization of the clathrin binding domain of nonvisual arrestins to the carboxy terminus. *J Biol Chem*, *272*(23), 15011-15016. https://doi.org/10.1074/jbc.272.23.15011

Kumari, P., Srivastava, A., Banerjee, R., Ghosh, E., Gupta, P., Ranjan, R., . . . Shukla, A. K. (2016). Functional competence of a partially engaged GPCR-beta-arrestin complex. *Nat Commun*, *7*, 13416. https://doi.org/10.1038/ncomms13416

Kumari, P., Srivastava, A., Ghosh, E., Ranjan, R., Dogra, S., Yadav, P. N., & Shukla, A. K. (2017). Core engagement with beta-arrestin is dispensable for agonist-induced vasopressin receptor endocytosis and ERK activation. *Mol Biol Cell*, *28*(8), 1003-1010. https://doi.org/10.1091/mbc.E16-12-0818

Kuna, R. S., Girada, S. B., Asalla, S., Vallentyne, J., Maddika, S., Patterson, J. T., . . . Mitra, P. (2013). Glucagon-like peptide-1 receptor-mediated endosomal cAMP generation promotes glucose-stimulated insulin secretion in pancreatic beta-cells. *Am J Physiol Endocrinol Metab*, *305*(2), E161-170. https://doi.org/10.1152/ajpendo.00551.2012

Laporte, S. A., Oakley, R. H., Zhang, J., Holt, J. A., Ferguson, S. S., Caron, M. G., & Barak, L. S. (1999). The beta2-adrenergic receptor/betaarrestin complex recruits the clathrin adaptor AP-2 during endocytosis. *Proc Natl Acad Sci U S A*, *96*(7), 3712-3717. https://doi.org/10.1073/pnas.96.7.3712

Ley, S. C., Marsh, M., Bebbington, C. R., Proudfoot, K., & Jordan, P. (1994). Distinct intracellular localization of Lck and Fyn protein tyrosine kinases in human T lymphocytes. *J Cell Biol*, *125*(3), 639-649. https://doi.org/10.1083/jcb.125.3.639

Lykke, K., Assentoft, M., Fenton, R. A., Rosenkilde, M. M., & MacAulay, N. (2015). Vasopressin receptors V1a and V2 are not osmosensors. *Physiol Rep*, *3*(8). https://doi.org/10.14814/phy2.12519

Moo, E. V., van Senten, J. R., Brauner-Osborne, H., & Moller, T. C. (2021). Arrestin-Dependent and -Independent Internalization of G Protein-Coupled Receptors: Methods, Mechanisms, and Implications on Cell Signaling. *Mol Pharmacol*, *99*(4), 242-255. https://doi.org/10.1124/molpharm.120.000192

Namkung, Y., Le Gouill, C., Lukashova, V., Kobayashi, H., Hogue, M., Khoury, E., . . . Laporte, S. A. (2016). Monitoring G protein-coupled receptor and beta-arrestin trafficking in live cells using enhanced bystander BRET. *Nat Commun*, *7*, 12178. https://doi.org/10.1038/ncomms12178

Namkung, Y., LeGouill, C., Kumar, S., Cao, Y., Teixeira, L. B., Lukasheva, V., . . . Laporte, S. A. (2018). Functional selectivity profiling of the angiotensin II type 1 receptor using pathway-wide BRET signaling sensors. *Sci Signal*, *11*(559). https://doi.org/10.1126/scisignal.aat1631

Nehme, R., Carpenter, B., Singhal, A., Strege, A., Edwards, P. C., White, C. F., . . . Tate, C. G. (2017). Mini-G proteins: Novel tools for studying GPCRs in their active conformation. *PLoS One*, *12*(4), e0175642. https://doi.org/10.1371/journal.pone.0175642

Nguyen, A. H., Thomsen, A. R. B., Cahill, T. J., 3rd, Huang, R., Huang, L. Y., Marcink, T., . . . Lefkowitz, R. J. (2019). Structure of an endosomal signaling GPCR-G protein-beta-arrestin megacomplex. *Nat Struct Mol Biol*, *26*(12), 1123-1131. https://doi.org/10.1038/s41594-019-0330-y

Nielsen, S., DiGiovanni, S. R., Christensen, E. I., Knepper, M. A., & Harris, H. W. (1993). Cellular and subcellular immunolocalization of vasopressin-regulated water channel in rat kidney. *Proc Natl Acad Sci U S A*, *90*(24), 11663-11667. https://doi.org/10.1073/pnas.90.24.11663

Oakley, R. H., Laporte, S. A., Holt, J. A., Barak, L. S., & Caron, M. G. (1999). Association of beta-arrestin with G protein-coupled receptors during clathrin-mediated endocytosis dictates the profile of receptor resensitization. *J Biol Chem*, *274*(45), 32248-32257. https://doi.org/10.1074/jbc.274.45.32248

Oakley, R. H., Laporte, S. A., Holt, J. A., Caron, M. G., & Barak, L. S. (2000). Differential affinities of visual arrestin, beta arrestin1, and beta arrestin2 for G protein-coupled receptors delineate two major classes of receptors. *J Biol Chem*, *275*(22), 17201-17210. https://doi.org/10.1074/jbc.M910348199

Okashah, N., Wright, S. C., Kawakami, K., Mathiasen, S., Zhou, J., Lu, S., . . . Lambert, N. A. (2020). Agonist-induced formation of unproductive receptor-G12 complexes. *Proc Natl Acad Sci U S A*, *117*(35), 21723-21730. https://doi.org/10.1073/pnas.2003787117

Pippig, S., Andexinger, S., Daniel, K., Puzicha, M., Caron, M. G., Lefkowitz, R. J., & Lohse, M. J. (1993). Overexpression of beta-arrestin and beta-adrenergic receptor kinase augment desensitization of beta 2-adrenergic receptors. *J Biol Chem*, *268*(5), 3201-3208. https://www.ncbi.nlm.nih.gov/pubmed/8381421

Pope, G. R., Tilve, S., McArdle, C. A., Lolait, S. J., & O'Carroll, A. M. (2016). Agonist-induced internalization and desensitization of the apelin receptor. *Mol Cell Endocrinol*, *437*, 108-119. https://doi.org/10.1016/j.mce.2016.07.040

Quoyer, J., Janz, J. M., Luo, J., Ren, Y., Armando, S., Lukashova, V., . . . Bouvier, M. (2013). Pepducin targeting the C-X-C chemokine receptor type 4 acts as a biased agonist favoring activation of the inhibitory G protein. *Proc Natl Acad Sci U S A*, *110*(52), E5088-5097. https://doi.org/10.1073/pnas.1312515110

Rose, A. S., Elgeti, M., Zachariae, U., Grubmuller, H., Hofmann, K. P., Scheerer, P., & Hildebrand, P. W. (2014). Position of transmembrane helix 6 determines receptor G protein coupling specificity. *J Am Chem Soc*, *136*(32), 11244-11247. https://doi.org/10.1021/ja5055109

Sandhu, M., Cho, A., Ma, N., Mukhaleva, E., Namkung, Y., Lee, S., . . . Vaidehi, N. (2022). Dynamic spatiotemporal determinants modulate GPCR:G protein coupling selectivity and promiscuity. *Nat Commun*, *13*(1), 7428. https://doi.org/10.1038/s41467-022-34055-5

Schwindinger, W. F., Fredericks, J., Watkins, L., Robinson, H., Bathon, J. M., Pines, M., . . . Levine, M. A. (1998). Coupling of the PTH/PTHrP receptor to multiple G-proteins. Direct demonstration of receptor activation of Gs, Gq/11, and Gi(1) by [alpha-32P]GTP-gamma-azidoanilide photoaffinity labeling. *Endocrine*, *8*(2), 201-209. https://doi.org/10.1385/ENDO:8:2:201

Shukla, A. K., Manglik, A., Kruse, A. C., Xiao, K., Reis, R. I., Tseng, W. C., . . . Lefkowitz, R. J. (2013). Structure of active beta-arrestin-1 bound to a G-protein-coupled receptor phosphopeptide. *Nature*, *497*(7447), 137-141. https://doi.org/10.1038/nature12120

Shukla, A. K., Westfield, G. H., Xiao, K., Reis, R. I., Huang, L. Y., Tripathi-Shukla, P., . . . Lefkowitz, R. J. (2014). Visualization of arrestin recruitment by a G-protein-coupled receptor. *Nature*, *512*(7513), 218-222. https://doi.org/10.1038/nature13430

Simonsen, A., Lippe, R., Christoforidis, S., Gaullier, J. M., Brech, A., Callaghan, J., . . . Stenmark, H. (1998). EEA1 links PI(3)K function to Rab5 regulation of endosome fusion. *Nature*, *394*(6692), 494-498. https://doi.org/10.1038/28879

Smith, J. S., Pack, T. F., Inoue, A., Lee, C., Zheng, K., Choi, I., . . . Rajagopal, S. (2021). Noncanonical scaffolding of G(alphai) and beta-arrestin by G protein-coupled receptors. *Science*, *371*(6534). https://doi.org/10.1126/science.aay1833

Taniguchi, M., Nagai, K., Arao, N., Kawasaki, T., Saito, T., Moritani, Y., . . . Tsukamoto, S. (2003). YM-254890, a novel platelet aggregation inhibitor produced by Chromobacterium sp. QS3666. *J Antibiot (Tokyo)*, *56*(4), 358-363. https://doi.org/10.7164/antibiotics.56.358

Thomsen, A. R. B., Plouffe, B., Cahill, T. J., 3rd, Shukla, A. K., Tarrasch, J. T., Dosey, A. M., . . . Lefkowitz, R. J. (2016). GPCR-G Protein-beta-Arrestin Super-Complex Mediates Sustained G Protein Signaling. *Cell*, *166*(4), 907-919. https://doi.org/10.1016/j.cell.2016.07.004

van der Westhuizen, E. T., Breton, B., Christopoulos, A., & Bouvier, M. (2014). Quantification of ligand bias for clinically relevant beta2-adrenergic receptor ligands: implications for drug taxonomy. *Mol Pharmacol*, *85*(3), 492-509. https://doi.org/10.1124/mol.113.088880

Van Eps, N., Altenbach, C., Caro, L. N., Latorraca, N. R., Hollingsworth, S. A., Dror, R. O., . . . Hubbell, W. L. (2018). Gi- and Gs-coupled GPCRs show different modes of G-protein binding. *Proc Natl Acad Sci U S A*, *115*(10), 2383-2388. https://doi.org/10.1073/pnas.1721896115

Wan, Q., Okashah, N., Inoue, A., Nehme, R., Carpenter, B., Tate, C. G., & Lambert, N. A. (2018). Mini G protein probes for active G protein-coupled receptors (GPCRs) in live cells. *J Biol Chem*, *293*(19), 7466-7473. https://doi.org/10.1074/jbc.RA118.001975

Wehbi, V. L., Stevenson, H. P., Feinstein, T. N., Calero, G., Romero, G., & Vilardaga, J. P. (2013). Noncanonical GPCR signaling arising from a PTH receptor-arrestin-Gbetagamma complex. *Proc Natl Acad Sci U S A*, *110*(4), 1530-1535. https://doi.org/10.1073/pnas.1205756110

Wright, S. C., Lukasheva, V., Le Gouill, C., Kobayashi, H., Breton, B., Mailhot-Larouche, S., . . . Bouvier, M. (2021). BRET-based effector membrane translocation assay monitors GPCR-promoted and endocytosis-mediated Gq activation at early endosomes. *Proc Natl Acad Sci U S A*, *118*(20). https://doi.org/10.1073/pnas.2025846118

Yang, M., He, R. L., Benovic, J. L., & Ye, R. D. (2009). beta-Arrestin1 interacts with the G-protein subunits beta1gamma2 and promotes beta1gamma2-dependent Akt signalling for NF-kappaB activation. *Biochem J*, *417*(1), 287-296. https://doi.org/10.1042/BJ20081561

Zacharias, D. A., Violin, J. D., Newton, A. C., & Tsien, R. Y. (2002). Partitioning of lipid-modified monomeric GFPs into membrane microdomains of live cells. *Science*, *296*(5569), 913-916. https://doi.org/10.1126/science.1068539

Zhu, X., Gilbert, S., Birnbaumer, M., & Birnbaumer, L. (1994). Dual signaling potential is common among Gs-coupled receptors and dependent on receptor density. *Mol Pharmacol*, *46*(3), 460-469. https://www.ncbi.nlm.nih.gov/pubmed/7935326

Zimmerman, B., Beautrait, A., Aguila, B., Charles, R., Escher, E., Claing, A., . . . Laporte, S. A. (2012). Differential beta-arrestin-dependent conformational signaling and cellular responses revealed by angiotensin analogs. *Sci Signal*, *5*(221), ra33. https://doi.org/10.1126/scisignal.2002522

Table 1

		AVP-induced maximal efficacy (ΔEbBRET ± SEM)	**Potency** ($LogEC_{50}$ ± SEM)
Plasma membrane	mGs Parental	0.324 ± 0.006	-7.90 ± 0.03
	mGs Δβarr1/2	0.376 ± 0.011**	-7.99 ± 0.04
	mGsq Parental	0.168 ± 0.005	-7.81 ± 0.04
	mGsq Δβarr1/2	0.180 ± 0.009	-7.95 ± 0.07
Early endosomes	mGs Parental	0.180 ± 0.004	-8.37 ± 0.03
	mGs Δβarr1/2	0.074 ± 0.004****	-8.34 ± 0.09
	mGsq Parental	0.050 ± 0.002	-8.38 ± 0.08
	mGsq Δβarr1/2	0.024 ± 0.002****	-8.32 ± 0.12

Parameters related to AVP dose-response curves of the mGs and mGsq recruitment to the plasma membrane or early endosomes in parental and Δβarr1/2 cells.
ΔEbBRET values were fitted using four parameters equation with the bottom fixed at zero. *n* = 4 biological replicates for each condition. Statistical differences between parental and Δβarr1/2 cells for AVP-induced maximal efficacy and potency were assessed by comparing independent fits with a global fit that shares the selected parameter using extra sum-of-squares F test (**$P \leq 0.01$, ****$P \leq 0.0001$).

Table 2

		AVP-mediated maximal efficacy (ΔEbBRET ± SEM)	**Potency** ($LogEC_{50}$ ± SEM)	**Transduction coefficient** (Logτ/Ka ± SEM)
mGs	PM V_2R	0.300 ± 0.018	-8.07 ± 0.10	7.98 ± 0.05
	PM $V_2\beta_2AR$	0.392 ± 0.025***	-8.07 ± 0.10	8.04 ± 0.08
	EE V_2R	0.167 ± 0.008	-8.65 ± 0.09	8.63 ± 0.11
	EE $V_2\beta_2AR$	0.150 ± 0.003	-8.34 ± 0.04**	8.31 ± 0.02*
mGsq	PM V_2R	0.161 ± 0.011	-7.88 ± 0.11	7.90 ± 0.10
	PM $V_2\beta_2AR$	0.183 ± 0.013	-7.97 ± 0.11	7.99 ± 0.10
	EE V_2R	0.050 ± 0.002	-8.44 ± 0.08	8.31 ± 0.03
	EE $V_2\beta_2AR$	0.061 ± 0.005*	-7.82 ± 0.14***	7.91 ± 0.17*

Parameters related to AVP dose-response curves of the recruitment of mGs and mGsq to the plasma membrane and early endosomes by the V_2R or $V_2\beta_2AR$.
ΔEbBRET values from the dose-response curves were fitted using four parameters equation with the bottom fixed at zero. *n* = 4 biological replicates for each condition. Statistical differences between V_2R and $V_2\beta_2AR$ for AVP-mediated maximal efficacy and potency were assessed by comparing independent fits with a global fit that shares the selected parameter using extra sum-of-squares F test (*$P \leq 0.05$, **$P \leq 0.01$, ***$P \leq 0.001$). Statistical differences between V_2R and $V_2\beta_2AR$ for Log(τ/Ka) values were assessed by two-way ANOVA and Sidak's post hoc test for multiple comparisons (*$P \leq 0.05$). PM, plasma membrane; EE, early endosomes.

Figure 1 with 1 supplement

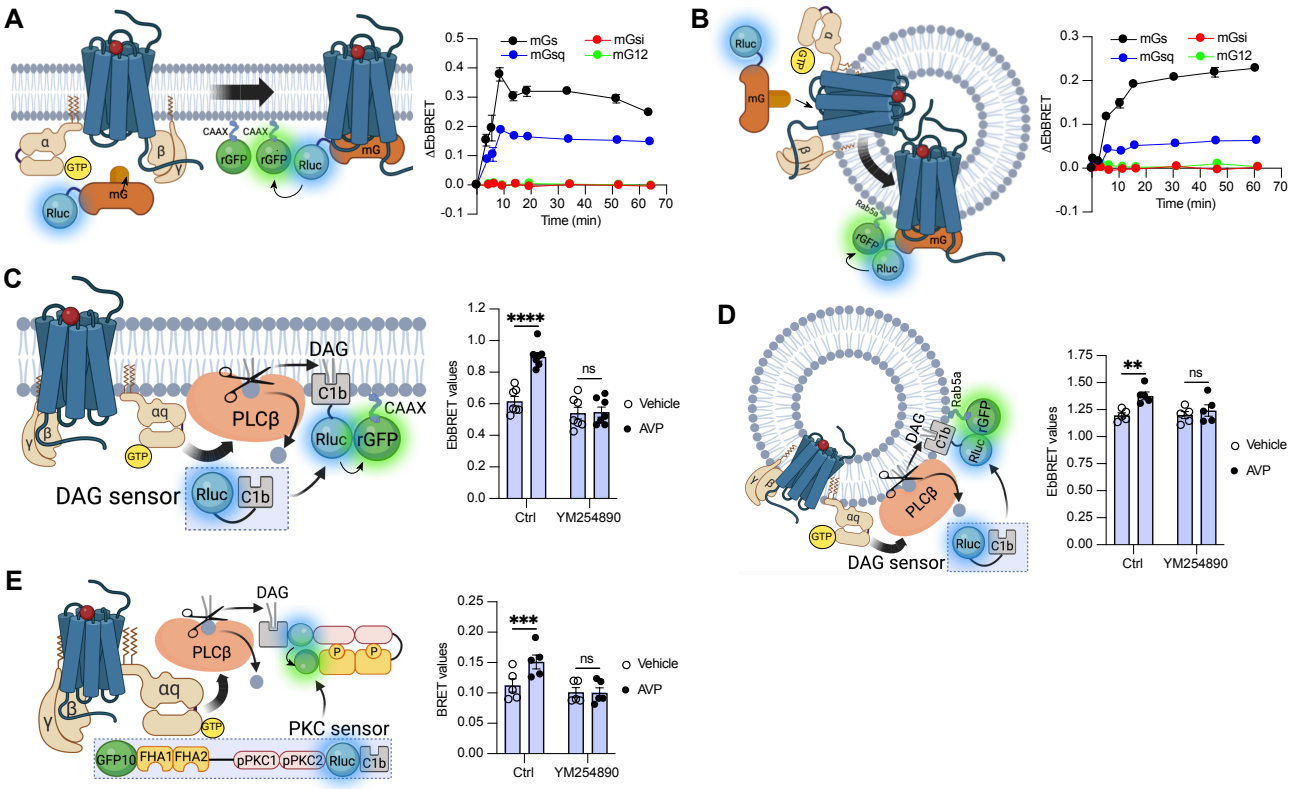

Activation of Gα$_s$ and Gα$_q$ at plasma membrane and early endosomes by V$_2$R monitored by BRET. **(A)** Left: Illustration of EbBRET biosensors used to monitor G protein activation at the plasma membrane. Right: Kinetics of the recruitment of mG proteins at the plasma membrane upon stimulation of V$_2$R with 1 μM AVP or vehicle. **(B)** Left: Illustration of EbBRET biosensors used to monitor G protein activation at the early endosomes. Right: Kinetics of the recruitment of mG proteins to early endosomes upon stimulation of V$_2$R with 1 μM AVP. **(C)** Left: Illustration of the BRET-based biosensor used to monitor DAG production at the plasma membrane. Right: DAG generated at the plasma membrane upon a 10 minute stimulation of V$_2$R with 1 μM AVP or vehicle in cells pre-treated 30 minutes with 0.1 μM YM254890 or vehicle. **(D;)** Left: Illustration of the BRET-based biosensor used to monitor DAG production at the early endosomes. Right: DAG generated at early endosomes upon a 10 minute stimulation of V$_2$R with 1 μM AVP in cells pre-treated 30 minutes with 0.1 μM YM254890 or vehicle. **(E)** Left: Illustration of the BRET-based PKC biosensor used to monitor PKC activation. Right: Activation of PKC upon 10 minutes of stimulation of V$_2$R with 1 μM AVP. For the kinetics, n = 3 (mGs, mGsi, and mGsq) or n = 4 (mG12) independent experiments. For the experiments using the DAG biosensor, n = 7 and n = 5 for measurements at plasma membrane and early endosomes, respectively. For the experiments using the PKC biosensor, n = 5. Asterisks mark statistically significant differences between vehicle and AVP treatments as assessed by two-way ANOVA and Sidak's post hoc test for multiple comparisons (**$P \leq 0.01$, ***$P \leq 0.001$, ****$P \leq 0.0001$).

Figure 2

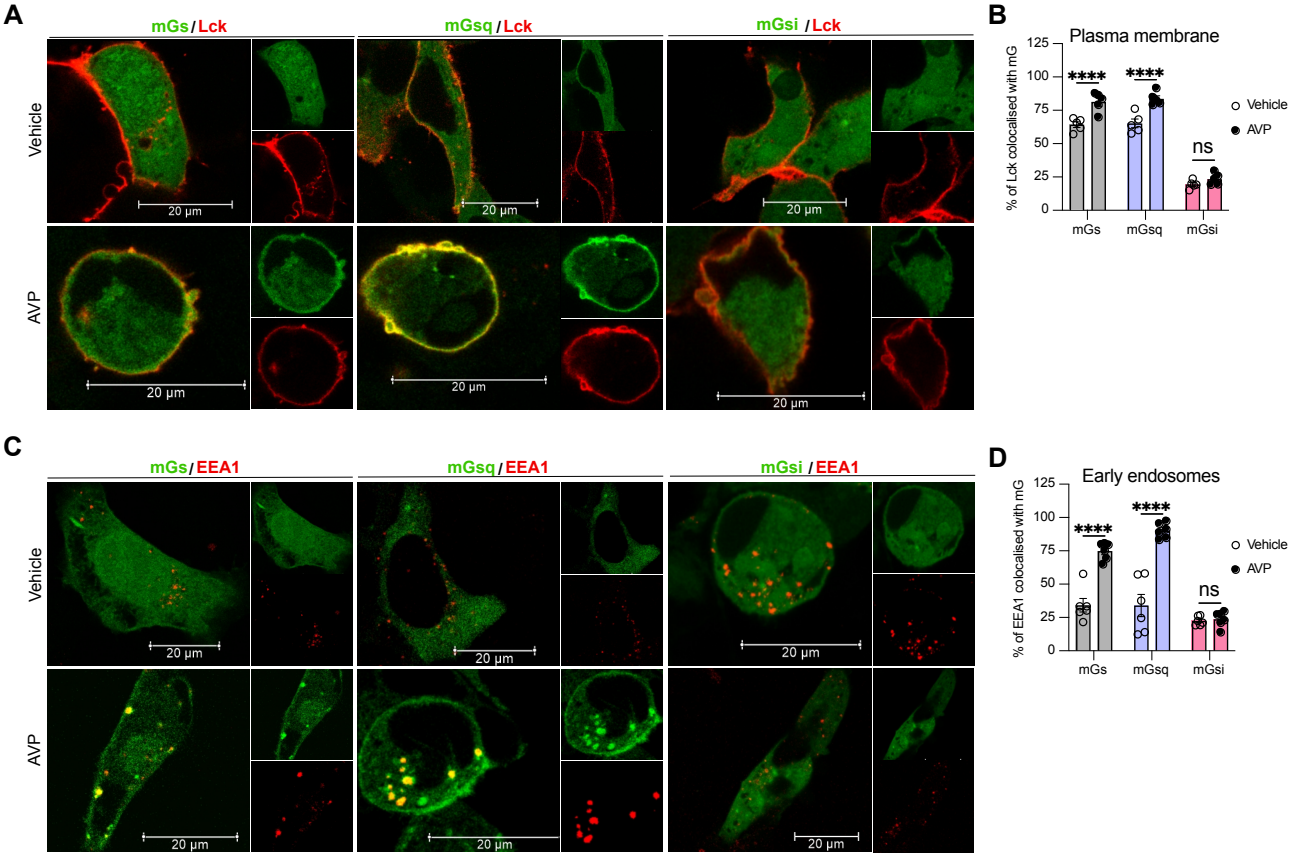

Activation of $G\alpha_s$ and $G\alpha_q$ at plasma membrane and early endosomes by V_2R monitored by confocal microscopy.
(A) Representative confocal microscopy images of cells expressing RFP-Lck, V_2R, and Halo-mGs (left panels), Halo-mGsq (middle panels), or Halo-mGsi (right panels) stimulated for 10 minutes with vehicle (upper panels) or 1 µM AVP (bottom panels). **(B)** Percentages of Lck colocalized with each Halo-mG calculated from 5 representative images. **(C)** Representative confocal microscopy images of cells expressing RFP-EEA1, V_2R, and Halo-mGs (left panels), Halo-mGsq (middle panels), or Halo-mGsi (right panels) stimulated for 45 minutes with vehicle (upper panels) or 1 µM AVP (bottom panels). **(D)** Percentages of EEA1 colocalized with each Halo-mG calculated from 6 representative images. n = 3 independent experiments for Lck and EEA1. Statistical differences between vehicle and AVP treatments were assessed by two-way ANOVA and Sidak's post hoc test for multiple comparisons (****$P \leq 0.0001$).

Figure 3 with 2 supplements

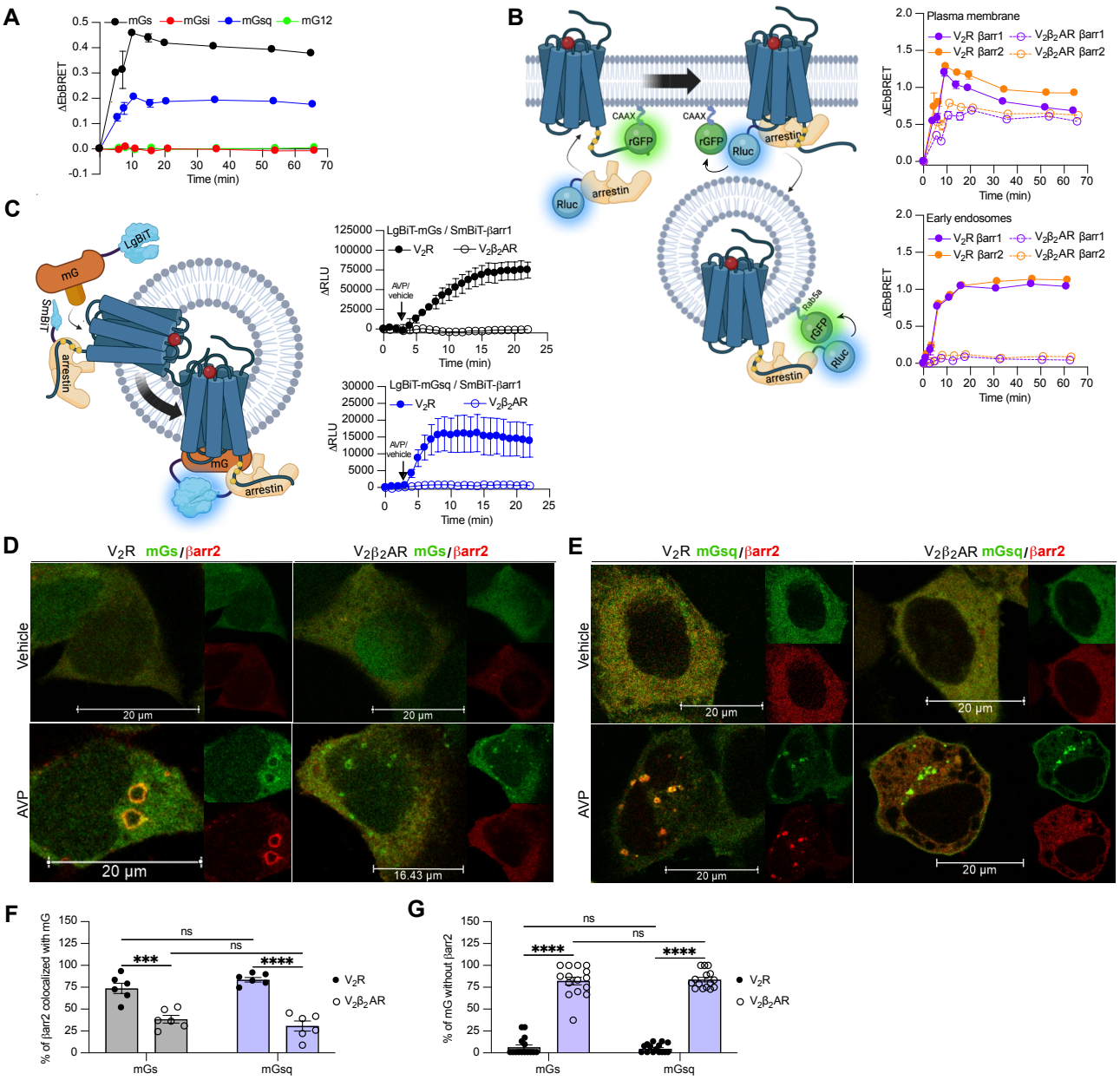

Formation of megaplexes with Gα$_s$ or Gα$_q$ upon stimulation with AVP.
(A) Kinetics of the recruitment of mG proteins at the plasma membrane upon stimulation of $V_2\beta_2$AR with 1 µM AVP. *n* = 3 for mGs, mGsi, and mGsq, and *n* = 4 for mG12. **(B)** Left: Illustration of the EbBRET biosensors used to monitor βarr recruitment to the plasma membrane and early endosomes. Right: Kinetics of the recruitment of βarr1 and βarr2 to the plasma membrane (upper panel) and to early endosomes (bottom panel) upon stimulation of V_2R or $V_2\beta_2$AR with 1 µM AVP. *n* = 3 for all conditions. **(C)** Left panel: Illustration of the nanoBiT biosensors used to monitor simultaneous coupling of Gα proteins and βarr1 to GPCRs. Right panels: Kinetics of the proximity between SmBiT-βarr1 and LgBiT-mGs (upper panel) or LgBiT-mGsq (bottom panel) upon stimulation of the receptors with 1 µM AVP. *n* = 3 for all conditions. **(D)** Representative confocal microscopy images of cells expressing Halo-mGs, strawberry-βarr2, and V_2R (left panels), or $V_2\beta_2$AR (right panels) and stimulated for 45 minutes with vehicle (upper panels) or 1 µM AVP (bottom panels). **(E)** Representative confocal microscopy images of cells expressing Halo-mGsq, strawberry-βarr2, and V_2R (left panels), or $V_2\beta_2$AR (right panels) and stimulated for 45 minutes with vehicle (upper panels) or 1 µM AVP (bottom panels). **(F)** Percentage of βarr2 colocalization with mGs or mGsq upon stimulation with 1µM AVP (6 representative images). **(G)** Percentage of mGs or mGsq puncta observed that were not colocalized with βarr2 upon stimulation with 1µM AVP (15 representative images). Asterisks mark significant differences between V_2R and $V_2\beta_2$AR assessed by two-way ANOVA and Sidak's post hoc test for multiple comparisons (***$P \leq 0.001$, ****$P \leq 0.0001$). No statistical difference (ns) was detected between mGs and mGsq.

Figure 4 with 4 supplements

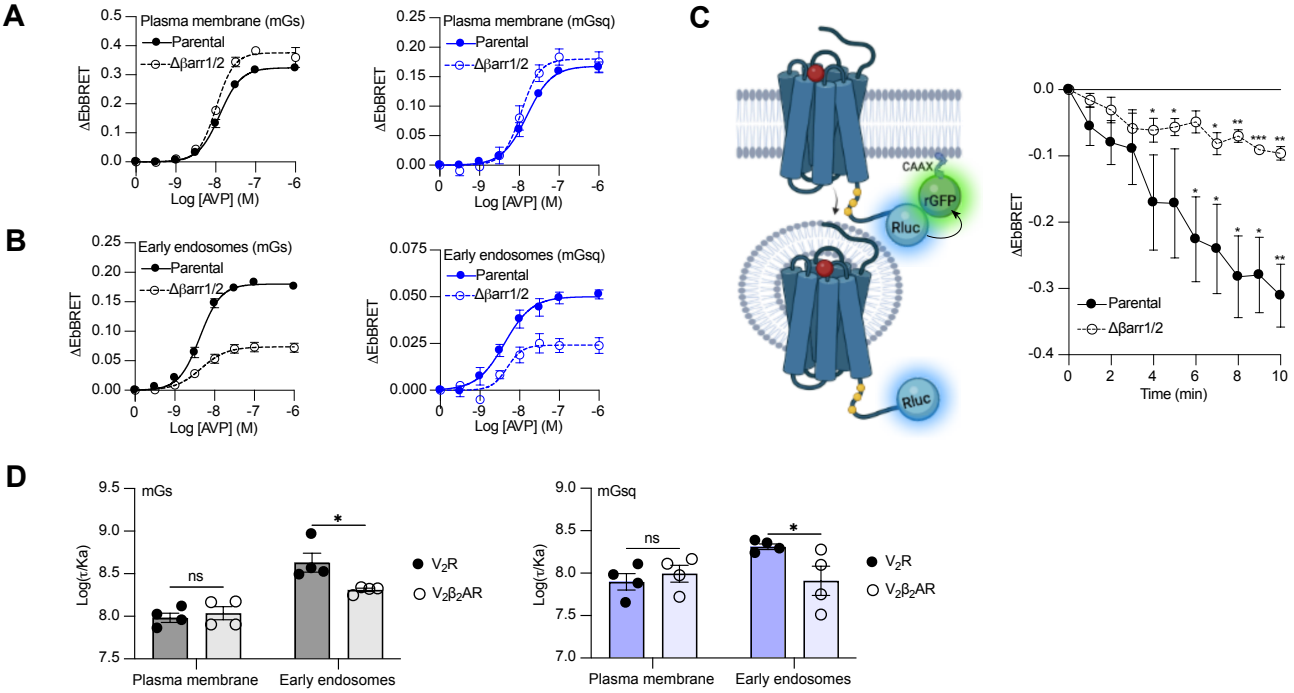

Contribution of megaplex to endosomal $G\alpha_s$ and $G\alpha_q$ signaling.
(A) AVP dose-response curves of the recruitment of mGs (left panel) and mGsq (right panel) to the plasma membrane in parental and Δβarr1/2 cells expressing V_2R upon 10 minutes of stimulation. **(B)** AVP dose-response curves of the recruitment of mGs (left panel) and mGsq (right panel) to early endosomes in parental and Δβarr1/2 cells expressing V_2R upon 45 minutes of stimulation. **(C)** Left: Illustration of EbBRET biosensors used to monitor AVP-mediated internalization of the V_2R. Right: Kinetics of V_2R internalization upon stimulation with AVP 0.1 μM. Asterisks mark significant differences from zero as assessed by one sample t test (*$P \leq 0.05$, **$P \leq 0.01$, ***$P \leq 0.001$). **(D)** Transduction coefficients of mGs (left panel) or mGsq (right panel) recruitment to the plasma membrane and early endosomes in V_2R- or $V_2\beta_2AR$-expressing cells. Asterisks mark significant differences between the V_2R and $V_2\beta_2AR$ as assessed by two-way ANOVA and Sidak's post hoc test for multiple comparisons (*$P \leq 0.05$). No statistical difference (ns) was detected between the V_2R and $V_2\beta_2AR$ at the plasma membrane. n = 4 biological replicates for all experiments.

Figure 5

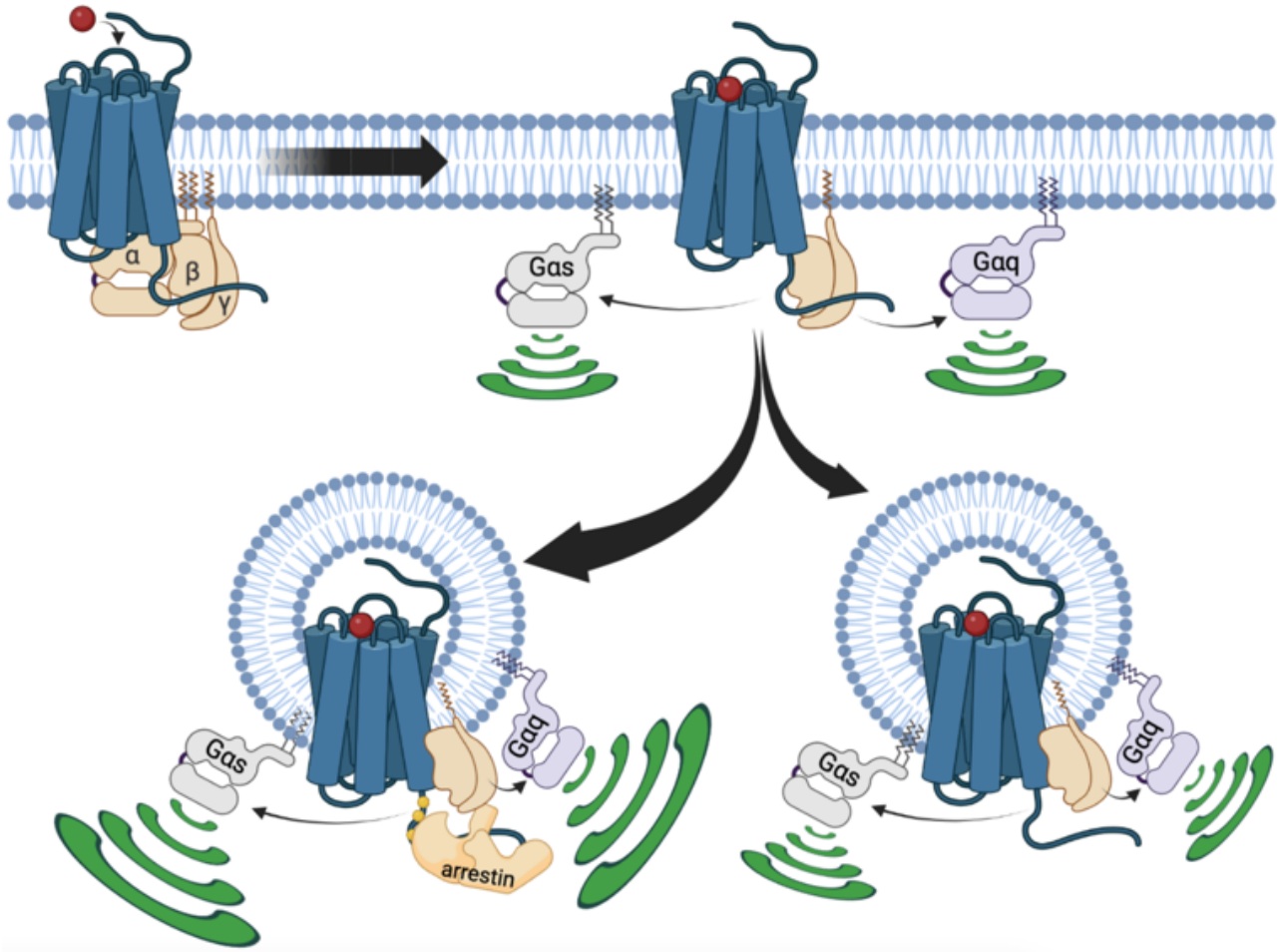

Updated model of V_2R signaling.
At the plasma membrane, AVP binding to V_2R results in receptor-mediated $G\alpha_s$ or $G\alpha_q$ activation. This initial G protein activation at the plasma membrane is followed by V_2R internalization into early endosomes. This internalization occurs primarily in a βarr-dependent manner, leading to the formation of a megaplex with $G\alpha_s$ or $G\alpha_{q/11}$ and robust activation of these G proteins from endosomes. Additionally, a minor population of V_2R internalize in a βarr-independent fashion, which also leads to minor but significant $G\alpha_s$ or $G\alpha_{q/11}$ activation from endosomes.